

Natural-background-oriented schlieren imaging

Michael John Hargather · Gary S. Settles

Received: 22 July 2008 / Revised: 26 June 2009 / Accepted: 29 June 2009
© Springer-Verlag 2009

Abstract The background-oriented schlieren (BOS) flow visualization method has the potential for large-scale flow imaging outside the laboratory by using natural backgrounds instead of the artificial patterns normally used indoors. The natural surroundings of an outdoor test site can sometimes be used as such a background, subject to criteria of fine scale, randomness and contrast that are developed here. Some natural backgrounds are more appropriate than others for a given application. Backgrounds used here to visualize both high- and low-speed schlieren disturbances include a sunlit cornfield and a backlit grove of trees. A range of image post-processing methods is considered for qualitative BOS. It is found that high sensitivity and a broad measuring range are in conflict here, much as they are in traditional schlieren instruments. Applications of natural-BOS include explosive characterization, firearms and artillery testing, chemical and natural-gas leak detection, and related phenomena.

1 Introduction

The use of traditional schlieren visualization methods is frequently limited by the small size and indoor location of the typical optical components employed. These limitations not only restrict the potential field-of-view of an experiment, but also prohibit the study of large equipment or phenomena that cannot typically fit into the laboratory. The background-oriented schlieren method, however, has

the potential to alleviate such limitations by allowing experiments outdoors.

Background-oriented schlieren (BOS) is the modern name for Hubert Schardin's simple background-distortion schlieren method of 1942 (Schardin 1942; Settles 2001). This technique allows refractive objects to be visualized by their distortion of a patterned background. The background distortion is directly related to the strength of the schlieren object as well as the optics and physical geometry of the experiment (Settles 2001). By comparing two images of the background, one with the schlieren object and one without, the density gradients within the schlieren object can be determined from the apparent shift in the background pattern (Venkatakrisnan and Meier 2004). The BOS technique can thus be used to measure two-dimensional density gradients within the field-of-view and then produce a tomographic reconstruction of the density field within the schlieren object (Meier 1999).

Koepf (1972) developed the first quantitative density measurements using this technique by measuring the displacement of a laser speckle pattern caused by a candle flame. Modern applications of BOS, using digital images and image processing, were pioneered by Meier (1999, 2002), followed by Dalziel et al. (2000) and Raffel et al. (2000). Dalziel et al. (2000) developed the technique, under the name "synthetic schlieren", by performing an extensive evaluation of the potential sensitivity and a variety of image processing techniques. Raffel et al. (2000) used a particle image velocimetry (PIV) analysis to measure pixel displacements, thus density gradients associated with the tip vortices of a helicopter in hover flight. In general, modern applications typically analyze digital image pairs through cross-correlation algorithms (Venkatakrisnan and Meier 2004; Meier 2002) or PIV software (Raffel et al. 2000; Richard and Raffel 2001) to determine

M. J. Hargather (✉) · G. S. Settles
Penn State Gas Dynamics Laboratory,
Pennsylvania State University, 301D Reber Building,
University Park, PA 16802, USA
e-mail: mjh340@psu.edu

the pixel shift caused by a schlieren object, thus the density gradients and density fields within the field-of-view.

Most often this approach uses modest laboratory-scale backgrounds of random dot patterns (Meier 2002). Meier (1999) first proposed using natural backgrounds in his patent. Richard and Raffel (2001), however, were the first to use “natural” BOS backgrounds when they used white paint splatter on concrete and a grassy field as backgrounds to visualize compressible vortices from helicopter rotors. More recent work by Kindler et al. (2007) used a range of natural backgrounds for the visualization of these compressible vortices. Kindler et al. also presented a statistical approach for quantifying the effectiveness of potential backgrounds.

Settles (2001, 1999b) reviewed outdoor schlieren and shadowgraph imaging in detail. Outdoor schlieren observation by background distortion was examined in particular, and several examples were given (blast wave seen against clouds, jet aircraft shock waves, and exhaust seen against a background tree-line or the sun, etc.). It was also shown that BOS is actually Schardin’s canonical schlieren method #1 (Schardin 1942). Readers are encouraged to see the pre-BOS historical survey in Settles (1999b), which is omitted here.

The present research explores the suitability of natural backgrounds for BOS visualization. Several natural backgrounds are used to visualize both high- and low-speed phenomena. A simple new approach is also found to process BOS image pairs in order to reveal pixel intensity changes qualitatively. Ultimately, these backgrounds and techniques are critiqued for their ability to render BOS visualizations and suggestions for the ideal natural background are presented.

2 Experimental setup

2.1 BOS sensitivity

Schardin’s schlieren method #1 (Schardin 1942; Settles 2001), being typical of BOS illumination, is illustrated in Fig. 1. Here, for simplicity, a single light–dark background boundary is shown. Point p in the schlieren object S refracts light through angle ε . This causes an apparent background shift or distortion of a point on the light–dark boundary to a point at p' . This shift is recorded by the camera.

The sensitivity of this system, i.e., the smallest density gradient that can be detected, is a function of the optical geometry shown in Fig. 1, the camera capability, and the strength of the schlieren object. For a given schlieren object, BOS sensitivity is influenced by the distance of the background to the object, $L - t$, and the distance L from

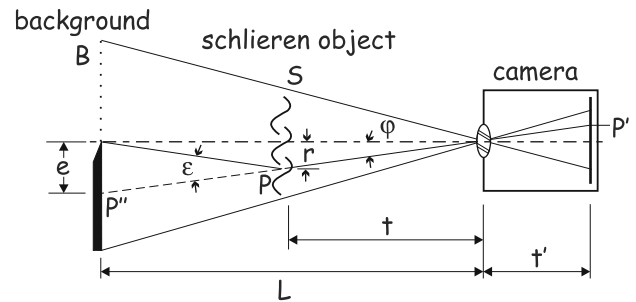


Fig. 1 Schardin’s schlieren method #1, the typical optical arrangement for BOS imaging

the background to the camera (Settles 2001; Meier 2002; Settles 1999b; Goldhahn and Seume 2007). Camera lens focal length and pixel size also affect the ability to detect small disturbances (Goldhahn and Seume 2007). In general, a distant background, imaged with a long-focal-length lens by a camera of high resolution (many small pixels) results in the greatest sensitivity.

The geometric setup is constrained, however, by depth-of-field, since maintaining both the background and schlieren object in reasonable focus is important. As the background pattern becomes defocused, it becomes impossible to image pixel distortions within the background image. As the schlieren object becomes defocused, the schlieren are no longer properly imaged. Thus, both the background and schlieren object must be in focus not only for good photography, but for accurate background distortion measurements.

For the present work, the required sensitivity was established by choosing a suitable distance $L - t$, then t was chosen for acceptable depth-of-field. This procedure usually places the schlieren object about halfway between the camera and the background.

2.2 Camera properties

Our principal camera is a high-speed digital black-and-white Photron APX-RS. For low-speed thermal plume imaging, this camera records images up to 3,000 frames per second (fps) with a $1,024 \times 1,024$ pixel resolution. High-speed images of gunshots and explosions were recorded at 15,000 fps with a pixel resolution of $1,024 \times 192$. The shutter speed was independently set in each case based on the ambient light conditions, but was at most $10 \mu\text{s}$ for the high-speed-imaging case. Even for low-speed events, using a high-speed camera was found beneficial in reducing errors due to background motion caused by the wind, etc., and shutter jitter.

The camera was fitted with a Nikon 80–200 mm variable zoom lens. The f/stop was adjusted to allow both the background and schlieren object to be more-or-less

simultaneously in focus. However, for all present BOS experiments the background was sharply focused while the subject was sometimes allowed to be slightly out-of-focus. Note that this conflicts with the philosophy espoused in (Settles 1999b), where a sharply focused subject and a fuzzy background were used.

A Nikon D80 digital SLR camera was also used for low-speed applications. This camera provided superior pixel resolution, thus potentially higher BOS sensitivity than the Photron APX-RS, but with limited control on the amount of time between images: typically about 1 s with the Nikon D80. Although the camera was firmly mounted in a tripod and triggered remotely to avoid camera motion between images, some shutter jitter still results, which can limit BOS sensitivity for some instances, where background shifts are less than 1 pixel in magnitude. Nevertheless, this consumer-grade digital camera was simple, portable, and effective for the low-speed outdoor BOS experiments.

2.3 Background selection

In the laboratory, random dot patterns can be easily generated and used as BOS backgrounds. A random dot pattern is ideal, providing high contrast and unique features from which image correlation algorithms can easily determine pixel shifts. In the field, though, creating such large artificial backgrounds is impractical. Instead, a natural background that exhibits the characteristics of a random dot pattern is desired: high contrast and random fine-scale structure.

The required background quality is also directly related to the object being visualized. For high-speed events, such as explosions, high background contrast is required to allow fast framing rates and brief shutter speeds. The needed contrast level also depends upon the analysis method or software to be used in processing the images. Background feature size limitations arise from the required schlieren resolution, and depend upon field-of-view, schlieren object strength, and image processing method. The background features must be large enough in the recorded images to allow the detection of pixel shifts. They must also be unique if image processing is to determine locations and their distortions accurately. Finally, background features need to be distributed uniformly; as demonstrated below, regions of low contrast or overlapped features result in the loss of data.

Two natural backgrounds are used here, the edge of a cornfield and a small grove of trees. The cornfield used here was approximately 3 m high and was illuminated directly by the sun. This produced detailed highlights and shadows having a unique semi-random pattern: on the scale of individual leaves randomness is achieved, but on a larger scale, groups of stalks nearly create a repeating pattern.

The grove of trees was approximately 30 m deep, allowing sufficient tree density while permitting sunlight transillumination from behind. On a winter afternoon in Central Pennsylvania the bare tree branches and trunks before the bright sky provided a high-contrast background with ample random detail. Various other natural backgrounds could also meet the above criteria, but are not explored here. A man-made background (corrugated steel silo) was also used in some experiments.

Another consideration for natural backgrounds is the importance of three-dimensional effects within the background. If a background has a significant variation in the location of features, thus causing significant variations in the schlieren-object-to-background length, three-dimensional effects would be expected. These three-dimensional effects will primarily result in variations in schlieren sensitivity within the image. A background with a significant variation in camera-to-background distance will also potentially be out-of-focus in some regions, resulting in reduced correlation effectiveness in those regions. The importance of these effects should be evaluated for a given scenario and geometric setup. The corn background used here was essentially two-dimensional, when the image processing was restricted to the corn height. The tree grove has some three-dimensional effects, although they are ignored here because only qualitative results are presented.

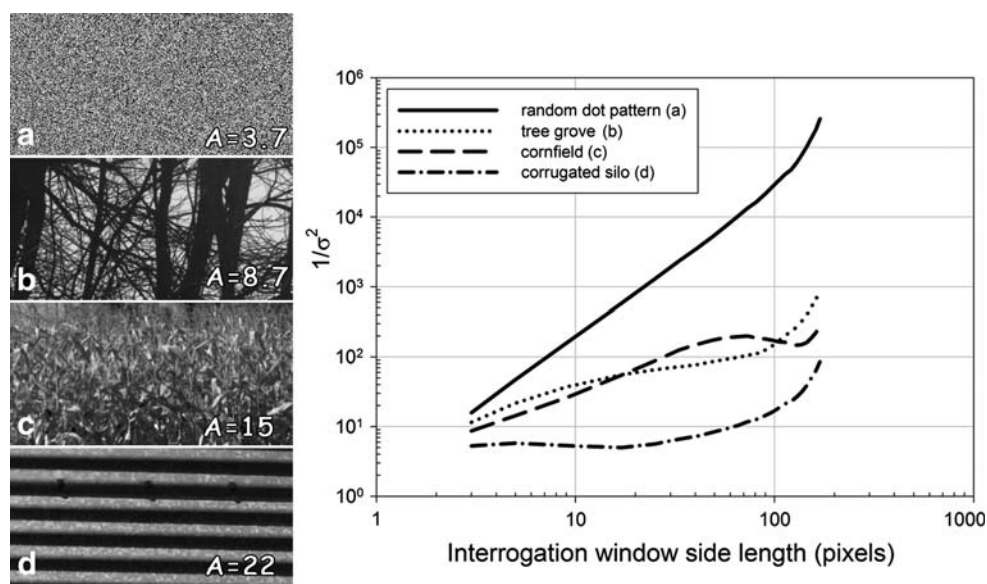
3 Experimental results

3.1 Background correlation analysis

A simple analysis, similar to that done by Kindler et al. (2007), was performed on each background to define a relative image correlation quality. The four images used for this analysis are shown in Fig. 2a–d, including one image of each natural background and one randomly generated dot pattern. For each image, cross correlations were performed between the entire image (381×191 pixels) and small interrogation windows selected from within the image. The side length of the square interrogation windows varied from 3 to 169 pixels.

A MATLAB algorithm calculated the normalized cross correlations between the image and each interrogation window using the function *normxcorr2*. Over 700 interrogation windows were randomly selected for each interrogation window size and the average results are presented here. For the normalized cross correlation, a value of 1 indicates a perfect correlation and that the location of the interrogation window was found exactly. The rest of the correlation values represent a degree of correlation, or noise in the ability to correlate accurately. The square of the standard deviation, σ^2 , of the correlation values

Fig. 2 Background images (a–d) and correlation results as a function of interrogation window size



throughout the image was used as a measure of the cross correlation effectiveness. The inverse of this, $1/\sigma^2$, is a measure of the signal-to-noise ratio for correlations throughout the image. The results, as a function of interrogation window size, are shown in Fig. 2.

The results of this analysis show general trends for the quality of each background. The random dot pattern always correlates better than the other backgrounds, as expected since it is ideal: random and high contrast. The corrugated silo always correlates the worst, with almost no improvement in correlation as a function of interrogation window size, until the window becomes a significant portion of the total image. This trend can be attributed to the regular pattern within the image, which creates many approximate correlation regions, thus a high noise level.

The cornfield and the tree grove images correlate similar to each other and better than the corrugated silo, but not as well as the random pattern. The decrease in the cornfield curve, near 100 pixel window length, can be attributed to a large-scale pattern within the corn that decreases the correlation quality when the window reaches a certain size. The tree grove correlation does not increase as rapidly as the cornfield or random dot pattern with increasing interrogation window size because of the large structures of the tree trunks. These regions are similar to the corrugation, and contribute significantly to the correlation noise. Ideally, the tree grove would contain more small branches which would lead to a more random, high-contrast background.

All of the data show an increasing correlation as the window size becomes a significant portion of the image; the last data point represents the case where the correlation window is 40% of the image area. Smaller interrogation windows, however, are able to detect smaller background

distortions, thus weaker schlieren disturbances. To effectively use these smaller interrogation windows, the images must have unique, fine-scale detail to allow sufficient correlation signal-to-noise ratio.

An estimate of the scale of the “structures” within each of the images of Fig. 2 was performed using the MATLAB function *watershed*. This function calculates the number of distinct regions within an image and outlines the “watershed pixel” boundaries between them. From this, the average number of pixels within each distinct region can be determined. This represents the average area, A , in pixels, of a “structure” for each image, and is given in Fig. 2a–d. As in typical PIV analysis, effective correlation and displacement detection is a function of both the structure and interrogation window sizes. The structure size in each image is directly related to the initial trends in the correlation effectiveness of each background: smaller structure size leads to more effective correlation at small interrogation window size. The analysis presented here typically used interrogation windows of 15–30 pixels in length.

3.2 Thermal plume from a hand-held propane torch

A commercial Bernz-o-Matic™ propane torch flame was used as an initial schlieren object to evaluate different background and image-processing options. The torch flame creates a strong local density gradient and a well-defined thermal plume of at least 1 m extent.

The first experiment performed with this torch used a corrugated steel silo as the background. With direct sunlight illumination this silo approximates the type of grid commonly used for the background-grid-distortion schlieren imaging that was classified by Schardin as his “schlieren method #2” (Schardin 1942; Settles 2001).

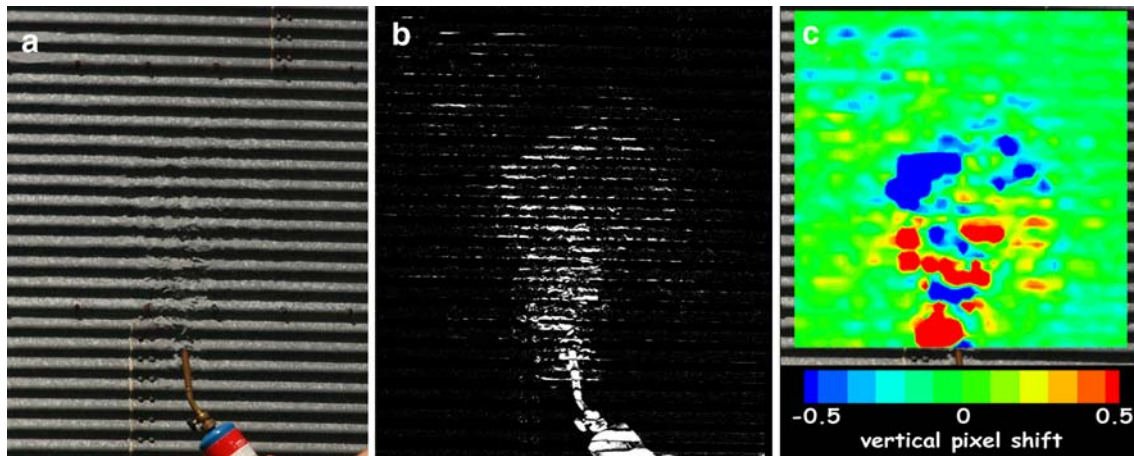


Fig. 3 Bernz-o-Matic™ propane torch visualized against a corrugated background. The raw image (a) is compared to a tare image to determine the pixel intensity change (b) and pixel shift (c)

Figure 3 shows three approaches to the visualization of the hot torch plume. The raw image, Fig. 3a, was taken with the Nikon D80 camera using distances t and $L - t$ both approximately 13 m. The torch plume can be seen as it distorts the boundaries of the corrugations. The pixel intensity change between the raw image and a tare image with no torch present is used to visualize the plume in Fig. 3b. The pixel shifts between the raw and tare images are then calculated using commercial PIV software to create Fig. 3c.

Figure 3b reveals the torch plume better than does the raw image (Fig. 3a). The image processing highlights locations where the pixel value has changed, i.e., where a schlieren disturbance exists, and the distracting background grid pattern is largely removed. Quantitatively, the intensity of each pixel in the processed image, denoted new , is determined from the pixel intensities in the *hot* and *cold* (raw and tare) images according to:

$$new(i, j) = \frac{(\text{hot}(i, j) - \text{cold}(i, j))^2}{\frac{\text{hot}(i, j) + \text{cold}(i, j)}{2} + 1} \quad (1)$$

The resulting processed image, Fig. 2b, shows only some residue of the corrugation pattern. Deflections are easily visualized along the edges of corrugation bands, but are difficult to observe in the center of the bands. Within the nearly black corrugation bands it is more difficult to detect small changes in the pixel intensity. Some false distortions are also observed along the light bands, which are thought to be noise due to sunlight illumination changes between images.

Figure 3c was created using Insight3G™ software from TSI, Inc. The software determines the pixel shift at each pixel location by matching patterns in the surrounding pixels. This PIV software is not intentionally designed for

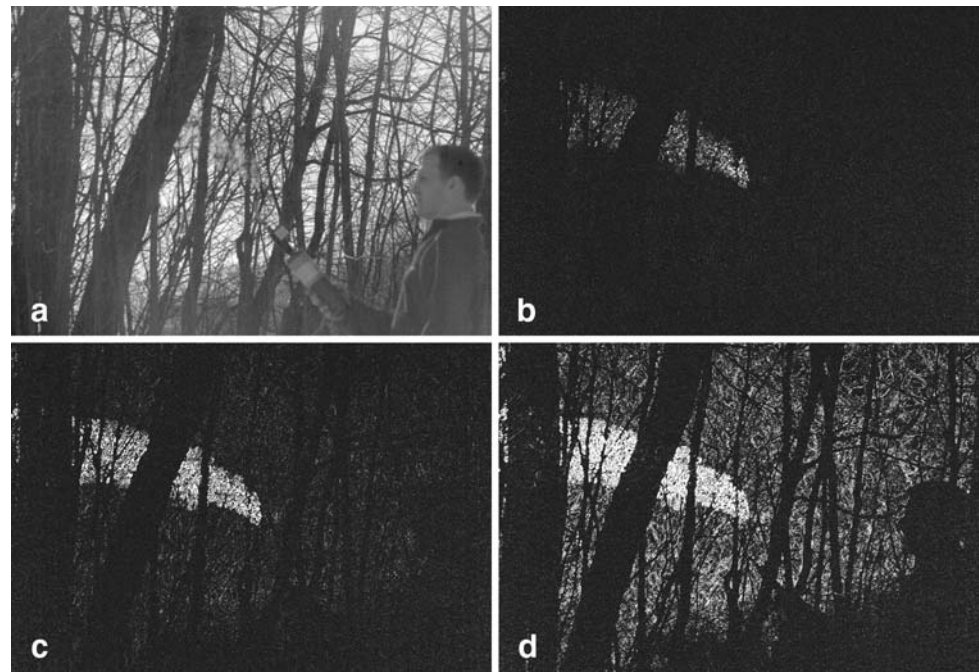
the BOS application, but it was nonetheless found useful for determining shifts as small as 0.05 pixel between images. This analysis with PIV software yields quantitative background distortions that can be used to define the density-gradient field within the flow as done elsewhere (Dalziel et al 2000; Venkatakrisnan and Meier 2004).

Overall, the corrugated steel succeeds conditionally as a BOS background even though it lacks the desired fine-scale random features. The horizontal features of the corrugation allow visualization of disturbances along the edge of the corrugation bands, similar to a horizontal knife-edge or other unidirectional schlieren cutoff-grid in more traditional schlieren approaches. While they are not naturally occurring, corrugated buildings can nonetheless serve as useful backgrounds for large-scale outdoor BOS imaging.

The grove of trees described in Sect. 3 was tried next. With the high-speed camera positioned approximately 40 m in front of the tree line, the propane torch was placed halfway between the camera and background and its plume was again visualized. Figure 4 shows the original image and field-of-view (Fig. 4a), along with three BOS images of the torch plume processed according to Eq. 1, and having time separations between images of 0.667 ms (Fig. 4b), 2 ms (Fig. 4c), and 10 ms (Fig. 4d).

In this case a tare image is not used; rather two subsequent images from the high-speed camera sequence are compared by the image analysis. By examining these sequential images, the time rate of change of the refractive index is visualized instead of the traditional spatial refractive index gradient found when a tare image is used. The present approach is more useful for natural BOS imaging where the background can change if images are separated by a large time duration. Some of the time variation can be eliminated by creating an average image from

Fig. 4 Images showing torch plume visualized against a background of trees transilluminated by the afternoon sunlight. The original image (a) is compared to images taken 0.667 ms (b), 2 ms (c), and 10 ms (d) later



a series of images, which can then be used as a tare image for individual image comparisons.

Figure 4b–d clearly shows a light wind carrying the torch plume right-to-left across each frame. Short time differences between these processed image pairs, e.g., Fig. 4b, help to limit background variations caused primarily by the wind shifting the trees. A longer time delay between images improves the plume visibility, which is linked to the timescale of the plume motion, but brings up the background noise as well, e.g., Fig. 4d. In that the plume is mixing with surrounding cold air, its refractions decrease with downstream distance and thus become less visible. Within limits, larger time delays between frames help maintain the plume visibility and better reveal its entire extent. Slower phenomena are also more easily visualized with larger time steps between the processed images. However, the ~ 1 s delay inherent in Nikon SLR camera images is too long to avoid excessive background motion, except perhaps in the case of perfectly calm wind conditions.

This natural tree background is more appropriate for present purposes than the corrugated steel used earlier because it has finer detail and a more random pattern. Areas in the background of the original image, Fig. 4a, having many thin branches at odd angles, reveal the plume well. The thicker tree trunks, however, cause a local loss of data due to the inability to determine pixel shifts in regions of featureless black background. With increased illumination of the trunks themselves, yielding textured surfaces, data might be obtained in these regions. This was not feasible, though, in the present series of experiments.

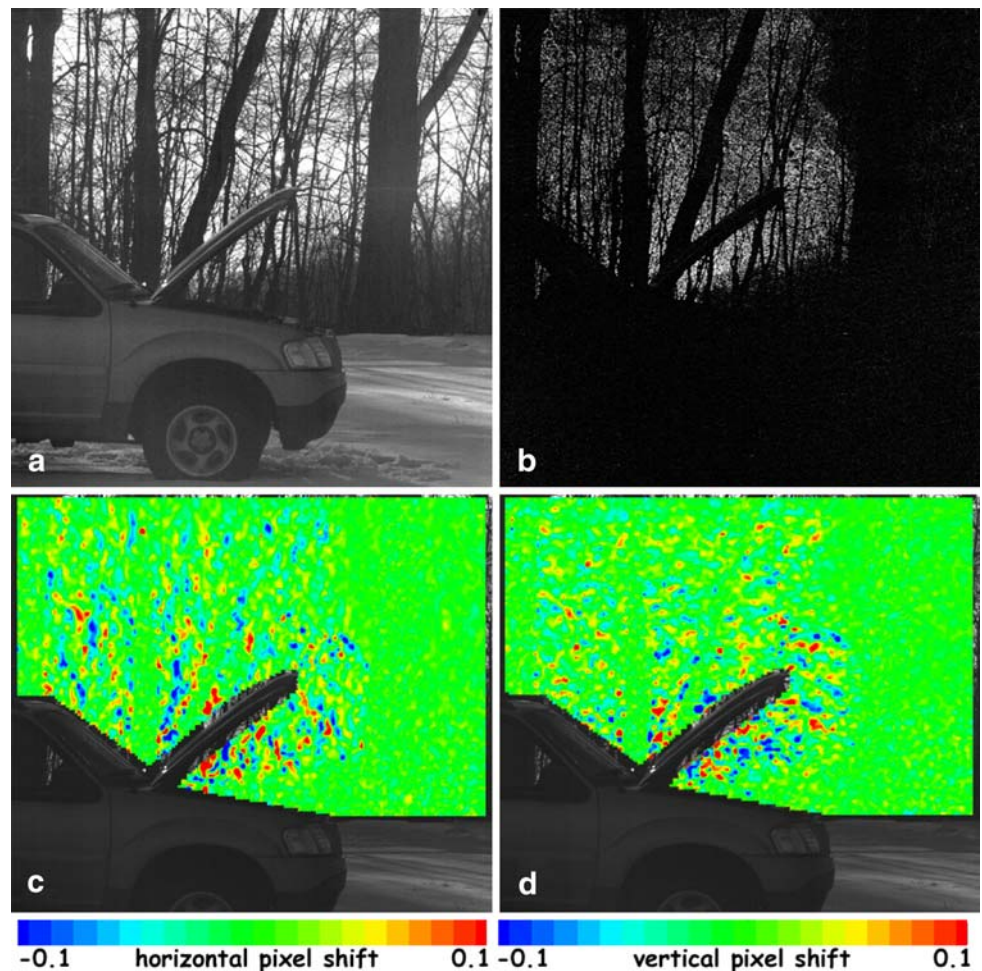
3.3 Thermal plume from a hot automobile engine

The tree background was also tried for the natural BOS visualization of a weaker thermal disturbance, the thermal plume rising from a hot automobile engine. Figure 5 shows the same tree-line background as before, but now with a truck at operating temperature with hood open in the schlieren-object position (20 m in front of the tree-line). The original image, Fig. 5a, is compared with an image obtained 100 ms later in Fig. 5b, where Eq. 1 has once again been used. The overall shape of the thermal plume rising from beneath the hood, and from the truck in general, is revealed. The same two images were also compared using the Insight3GTM software in Fig. 5c, d.

Based on Fig. 5, the weak truck plume is difficult to visualize with the present background and sensitivity level. The Insight3GTM software also reveals the gross outline of the plume without showing any coherent plume structure. Both horizontal (Fig. 5c) and vertical (Fig. 5d) pixel shifts are shown, though little difference can be seen between them. In general, the pixel shift direction should be selected in the same manner as one would choose a horizontal or vertical knife-edge orientation in conventional schlieren imaging (Settles 2001). The Insight3GTM software is most effective where unique background features are present, but also fails across the largest tree trunks. This weak-plume visualization could be improved with more sensitivity and a better tree-line background, but the latter was not attempted here.

Instead, the sun-illuminated cornfield described earlier was found to be a more appropriate background for this

Fig. 5 BOS images showing the thermal plume of a hot truck visualized against a background of trees. The original image (a) is compared with an image taken 100 ms later to determine the pixel intensity change (b), and the horizontal (c) and vertical (d) pixel shifts



schlieren object. In bright sunlight the corn provides a near-random natural pattern of light and dark patches that is ideal for BOS. The height of the corn, approximately 3 m, limits the vertical field-of-view but the horizontal field-of-view can be many meters long. For visualizing the truck plume, the camera was positioned at approximately $L = 75$ m from the corn-row background and the truck was again located approximately halfway between the two. Note that this almost doubles the previous tree-line BOS sensitivity, based on the geometrical optics of Fig. 1.

Figure 6 shows the truck and the corn background in the original image (Fig. 6a), and the pixel shift (Fig. 6b) between that image and one recorded 7 ms later, as determined by the Insight3GTM software. Now the thermal plume is clearly seen rising from the engine compartment. Other thermal plumes also rise from the truck aft of the engine compartment. This increased sensitivity, relative to that of Fig. 5, reveals more physics of the flow and is ascribed to doubling $L - t$ and a better natural background.

In order to visualize this weak plume by BOS, an ideal background and high sensitivity are called for. The cornfield background used here is near-ideal because of its high

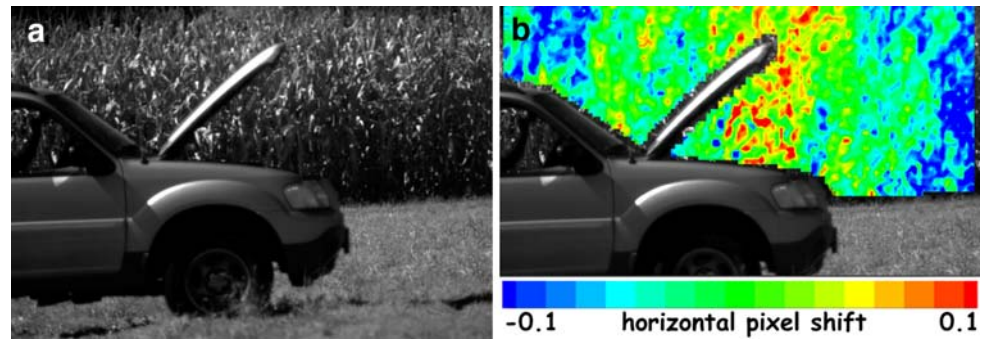
contrast and randomly detailed texture. Even so, additional sensitivity obtained by increasing the distance $L - t$ between Figs. 5 and 6 visibly improves the visualization. A high-speed digital camera was also required here to limit background motion, thus false distortions, between images, especially for the case of the corn leaves which were susceptible to the breeze.

3.4 Shock waves in the discharge of a 0.30-06 rifle

A high-powered 0.30-06 rifle is next used to explore the potential for high-speed visualization of shock waves using the BOS technique with natural backgrounds. This rifle discharge has been previously visualized using the Penn State Gas Dynamics Lab's Full-Scale Schlieren system (Settles and Dodson 2005). The goal of the present work is to reproduce this visualization with a cornfield background.

The cornfield was again illuminated by direct sunlight and the camera was placed at approximately $L = 25$ m from the corn row with the subject located midway between the two. The corn was selected here for its near-ideal background properties, even though the large

Fig. 6 Image showing a hot truck engine plume visualized against a background of corn. The original image (a) is compared to one recorded 7 ms later to determine the horizontal pixel shift (b)



refractive disturbance of the muzzle blast was not expected to require ultimate schlieren sensitivity. The camera shutter speed setting was $10 \mu\text{s}$, the fastest speed available while still maintaining sufficient exposure of the subject and background, and images were obtained at 15,000 fps.

Figure 7a shows an image recorded approximately 0.67 ms after the bullet emerges from the gun barrel. This image is compared with a “tare” image taken immediately before the bullet emerges from the barrel in Fig. 7b, where the intensity differencing scheme of Eq. 1 is once again applied. The horizontal pixel shift between the two images, computed by the Insight3G™ software, is shown in Fig. 7c. Finally, a Full-Scale Schlieren System image of the 0.30-06 rifle discharge (Settles and Dodson 2005; Settles 2006) is shown in Fig. 7d for comparison.

Given only the image in Fig. 7a, the eye can discern little more than some muzzle flash and distortion. The pixel-intensity-difference image, Fig. 7b, shows the spherical muzzle-blast shock wave, the emerging propellant gases and the bullet, but fails to clearly show the oblique shock waves streaming back from the bullet. The high background noise level characteristic of such images sets a limit on the visible detail.

The pixel shift image, Fig. 7c, reveals the muzzle blast well, but is not sensitive enough to capture either the bullet or its oblique shocks. It does, however, yield pixel-shift direction information in color that is lacking in Fig. 7b. This image also shows the importance of selecting the sensitivity required for a given application. The distortions measured here include some regions with large pixel distortions that effectively over-ranged the PIV software’s ability to accurately determine a finite pixel shift. The potential over-ranging is a significant problem for quantitative data reduction, but is not addressed in the present qualitative study.

In all these images some shock wave blurring (at least several mm) occurs due to the $10 \mu\text{s}$ shutter speed used here. Better illumination or a faster camera lens, by providing a shorter exposure, would allow sharper BOS images without requiring a significant sensitivity increase.

Finally, it is obvious that none of the natural BOS images can compete with Fig. 7d in terms of resolution,

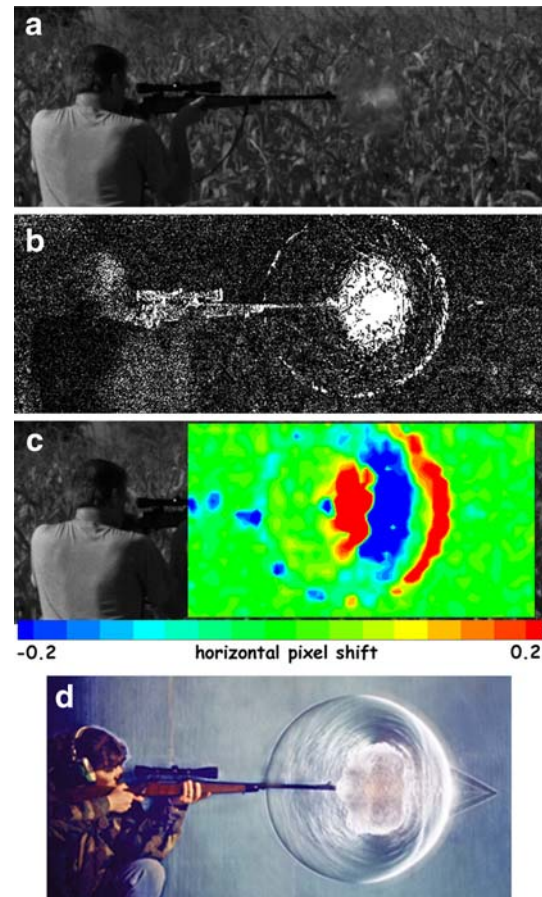


Fig. 7 High-speed images of a 0.30-06 rifle discharge showing the muzzle blast and supersonic bullet. A raw image (a) is compared with a tare image to find the pixel intensity change (b) and the horizontal pixel shift (c). The BOS images b and c show different views of the gunshot also imaged using the PSGDL Full-Scale Schlieren system (d) (Settles and Dodson 2005; Settles 2006)

sensitivity, or visual appeal. Note, however, that this Full-Scale Schlieren image was taken in a large indoor facility that was developed over a period of several years with the expenditure of considerable time, effort and money (Settles 2001; Settles 2006, 2004; Settles and Dodson 2005), whereas Fig. 7a–c were shot during an excursion to a country cornfield on a sunny afternoon.

3.5 Shock waves from an explosion

Since the cornfield background has proven the most successful so far, it is used for a final example of natural BOS imaging using a 1-g charge of triacetone triperoxide (TATP), a primary explosive. This charge was exploded and imaged using the same camera settings and physical distances as in the previous section, so the schlieren sensitivity remains unchanged. The explosive charge was suspended on a wooden stake in the field-of-view, as can be seen in Fig. 8a.

The intensity images in Fig. 8b–d show the shock wave propagating out from the explosion center. These images also show disturbances caused by the gaseous fireball of the explosion. This technique could be used to track the spherical shock wave propagation away from the explosion center in order to characterize the explosive yield, as was previously done by shadowgraphy (Hargather and Settles 2007).

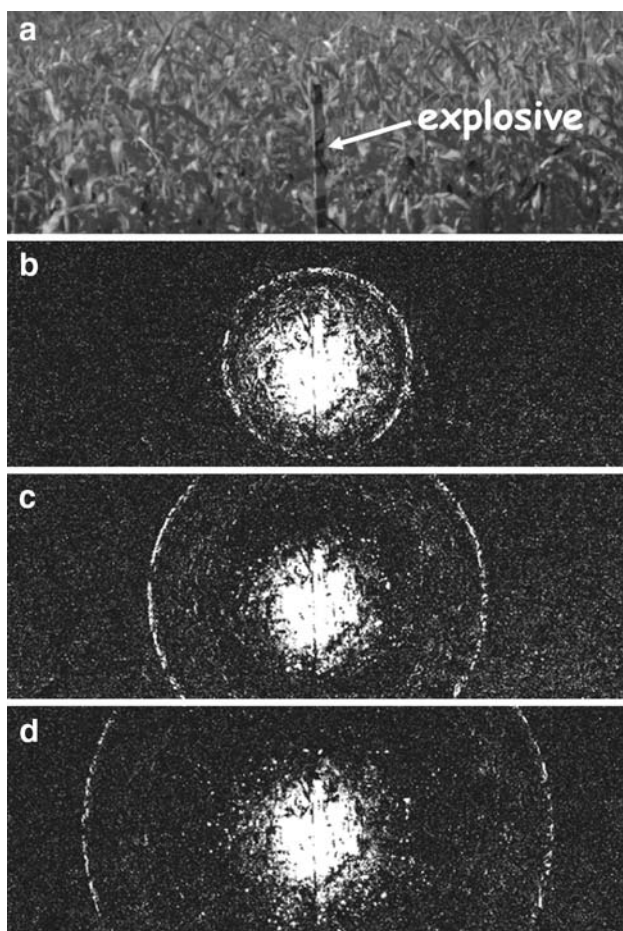


Fig. 8 Images of a 1 g TATP explosion showing shock propagation. Pixel-intensity-difference images are obtained from reference frame (a) and later images at times of 0.67 ms (b), 1.33 ms (c), and 2.0 ms (d) after the explosion

The same characterization process could then be applied to field tests of large explosive charges that cannot be safely tested in the laboratory, but can be exploded at an outdoor range with an appropriate natural background for BOS imaging.

4 Conclusions

Background-oriented schlieren is not a new idea, having doubtless been observed outdoors long before it was described by Hooke, Mach, and Schardin (Settles 2001). The relatively new BOS visualization method likewise has the potential for flow visualization outside the laboratory using natural backgrounds. The natural surroundings of an outdoor test site, for example, can be used as a background against which to examine pixel shifts caused by schlieren effects produced during the testing. By taking advantage of such natural backgrounds, some of the size and cost limitations of BOS imaging can be overcome.

The choice of a natural background, however, requires one to consider both the nature of the phenomenon to be visualized and the requirements of the image processing method to be used in data reduction. For typical BOS image processing, an ideal background consists of small, high-contrast, randomly distributed features. The desired background feature size is directly related to the schlieren object distortion strength, since schlieren distortions should be about the same size as the background features. Of the two natural backgrounds used here, appropriate feature size was demonstrated by a cornfield while a backlit tree grove caused data loss in some locations where there were thick tree trunks.

Effective BOS visualization outdoors also requires an optical setup, though a simplistic one, that is chosen to effectively visualize the disturbance of interest. For weak disturbances, a long object-to-background distance is needed for schlieren sensitivity. This usually implies a long camera-to-object distance as well, in order to maintain sharp focus of both the object and the background. Selecting an appropriate camera and lens combination is also important: we found that a long-focal-length lens and a digital camera with large pixel resolution provided the maximum BOS sensitivity once the object-to-background distance was set.

A typical BOS experimental setup is constrained by the required field-of-view and the illumination requirements of the available camera. With fixed camera resolution, the camera-to-background distance is first determined in order to obtain an appropriate pixel shift against the desired background. The schlieren object is then located in the field-of-view approximately midway between the camera

and background in order to maximize sensitivity while maintaining sharp focus.

Following the experiment, the resulting images are processed to highlight pixel changes between image pairs caused by the schlieren object. The choice of image processing technique depends on the desired result, and can be the most involved part of the process if quantitative pixel-shift data are desired. A simple pixel-intensity-differencing algorithm was shown effective here for qualitative natural-BOS imaging. Commercial particle image velocimetry software was also applied to measure sub-pixel shifts quantitatively. The quantitative approach is, however, limited when the background distortion exceeds a certain threshold, demonstrating that BOS, like traditional schlieren, suffers a compromise between high sensitivity and a broad measuring range (Settles 2001).

High-speed outdoor BOS imaging imposes further constraints: digital cameras like the one used here lose pixel resolution by segmenting the sensor array as the frame rate increases. Further, the need for short exposure times at high frame rates demands strong illumination and high background contrast. In reality, image underexposure becomes likely at high frame rates; it occurred in the present experiments, but was correctable after the test by image post-processing.

The natural-BOS results obtained here do not have the fine, almost-artistic quality attainable in laboratory schlieren images. On the other hand, no refined optics are required beyond the camera and its lens, and a large field-of-view is had without needing a Palomar-scale parabolic mirror. In the spirit of Hooke, Mach, and Schardin, the present approach takes advantage of backgrounds and illumination already supplied by nature.

Overall, natural-BOS imaging can be used in a variety of outdoor applications where the typical methods of optical flow visualization cannot be applied. It mainly requires sufficient physical space, camera resolution and speed, and proper image-processing routines. Applications that have yet to be tried include full-scale explosives field testing, external artillery ballistics, and chemical and natural-gas leak detection (Peale and Summers 1996; Settles 1999a), to name a few. Other potential natural and quasi-natural backgrounds, yet to be tested, include striated canyon walls and cliffs, the mottled background of the desert, quarry-stone fills, and stucco and split-face masonry walls in oblique sunlight.

Acknowledgments Authors owe their special thanks to L. J. Dodson-Dreibelbis, J. D. Miller, and T. J. Liebner.

References

- Dalziel S, Hughes G, Sutherland B (2000) Whole-field density measurements by 'synthetic schlieren'. *Exp Fluids* 28(4):322–335
- Goldhahn E, Seume J (2007) The background oriented schlieren technique: sensitivity, accuracy, resolution and application to a three-dimensional density field. *Exp Fluids* 43(2–3):241–249
- Hargather MJ, Settles GS (2007) Optical measurement and scaling of blasts from gram-range explosive charges. *Shock Waves* 17:215–223
- Kindler K, Goldhahn E, Leopold F, Raffel M (2007) Recent developments in background oriented schlieren methods for rotor blade tip vortex measurements. *Exp Fluids* 43(2–3):233–240
- Koepf U (1972) Application of speckling for measuring the deflection of laser light by phase objects. *Opt Commun* 5(5):347–350
- Meier GEA (1999) Hintergrund schlierenmessverfahren. Deutsche Patentanmeldung, DE 199 42 856 A1
- Meier GEA (2002) Computerized background-oriented schlieren. *Exp Fluids* 33(1):181–187
- Peale R, Summers P (1996) Zebra schlieren optics for leak detection. *Appl Optics* 35(22):4518–4521
- Raffel M, Richard H, Meier GEA (2000) On the applicability of background oriented optical tomography for large scale aerodynamic investigations. *Exp Fluids* 28(5):477–481
- Richard H, Raffel M (2001) Principle and applications of the background oriented schlieren (BOS) method. *Meas Sci Technol* 12(9):1576–1585
- Schardin H (1942) Die schlierenverfahren und ihre anwendungen. *Ergebnisse der Exakten Naturwissenschaften* 20:303–439
- Settles GS (1999a) Imaging gas leaks by using schlieren optics. *Pipeline Gas J* 226(9):28–30
- Settles GS (1999b) Schlieren and shadowgraph imaging in the great outdoors. In: Mochizuki S (ed) 2nd Pacific symposium on flow visualization and image processing. Honolulu, USA
- Settles GS (2001) Schlieren and shadowgraph techniques: visualizing phenomena in transparent media. Springer, Berlin
- Settles GS (2004) The Penn State full-scale schlieren system. In: Mueller T, Grant I (eds) Proceedings 11th international symposium on flow visualization. Notre Dame University, USA
- Settles GS (2006) High-speed imaging of shock waves, explosions, and gunshots. *Am Sci* 94(1):22–31
- Settles GS, Dodson LJ (2005) Full-scale schlieren visualization of supersonic bullet and muzzle blast from firing a 0.30-06 rifle. *J Visual-Japan* 8(1):6
- Venkatakrisnan L, Meier GEA (2004) Density measurements using the background oriented schlieren technique. *Exp Fluids* 37(2):237–247